

# The light-by-light contribution to the muon anomalous magnetic moment from the axial-vector mesons exchanges within the nonlocal quark model

A.E. Radzhabov,<sup>1</sup> A.S. Zhevlakov,<sup>1,2</sup> A.P. Martynenko,<sup>3</sup> and F.A. Martynenko<sup>3</sup>

<sup>1</sup>*Matrosov Institute for System Dynamics and Control Theory SB RAS, 664033, Irkutsk, Russia*

<sup>2</sup>*Joint Institute of Nuclear Research, BLTP, 141980, Moscow region, Dubna, Russia*

<sup>3</sup>*Samara University, 443086, Samara, Russia*

Contribution of axial-vector mesons to anomalous magnetic moment of muon through light-by-light process is considered in the framework of nonlocal quark model. The model is based on four-quark interaction with scalar–pseudoscalar and vector–axial-vector sectors. While transversal component of axial-vector corresponds to spin-1 particle the unphysical longitudinal component is mixed with pseudoscalar meson. The model parameters are refitted to the pion properties in the presence of  $\pi - a_1$  mixing. The total estimation for  $a_1 + f_1$  mesons light-by-light contribution is  $(3.6 \pm 1.8) \cdot 10^{-11}$ .

## I. INTRODUCTION

Anomalous magnetic moments  $a = (g - 2)/2$  (AMM) of electron and muon are measured with unprecedented accuracy for physics of elementary particles. The experimental value for electron anomaly measured with a one-electron quantum cyclotron is (in units  $10^{-11}$ )[1]

$$a_e^{\text{exp}} = 115965218.073 \pm 0.028 \times 10^{-11}. \quad (1)$$

The value for  $a_\mu = (g - 2)/2$  was measured at Brookhaven National Laboratory [2] and Fermilab [3] experiments and weighted average are

$$\begin{aligned} a_\mu^{\text{BNL}} &= 116592089 \pm 63 \times 10^{-11}, \\ a_\mu^{\text{FNAL}} &= 116592040 \pm 54 \times 10^{-11}, \\ a_\mu^{\text{exp}} &= 116592061 \pm 41 \times 10^{-11}. \end{aligned} \quad (2)$$

On the other hand, leptons magnetic moments can be estimated in the framework of the Standard Model, see e.g. [4] and [5], and therefore one can check our understanding of interactions around. While electron anomaly is mostly due to electromagnetic interactions (hadronic contribution to electron anomaly estimated to be only  $0.1693 \cdot 10^{-11}$  [4]), the muon one represents the challenge to theoreticians for correct descriptions since it is more sensitive to strong, weak and possible new physics contributions. The difference between experimental measurement and theoretical prediction of muon magnetic anomaly is exciting physicists for a long time as a possible hint that seems there is new physics beyond Standard Model (SM) which can be discovered even at low energies with high precision experiment. Nowadays this difference is estimated to be [6]

$$a_\mu^{\text{exp}} - a_\mu^{\text{SM}} = 251 \pm 41 \pm 43 \times 10^{-11}. \quad (3)$$

In SM the  $a_\mu$  comes from electromagnetic, strong and weak interactions, which contributes at orders  $10^{-2}$ ,  $10^{-6}$  and  $10^{-8}$ . The theoretical understanding of  $a_\mu$  is mostly limited due to strong sector. This is due to nonperturbative nature of quantum chromodynamics (QCD), i.e. at low energies the strong coupling constant is not a small parameter. Therefore the estimations for the leading order strong contribution on the base experimental data of electron-positron annihilation to hadrons is classically used. Last years there appears also the lattice QCD estimations. The whole story can be found in "White paper" 2020 to which we refer careful readers [5].

The light-by-light (LbL) contribution via nonperturbative QCD vacuum is suppressed in compared with the hadronic vacuum polarization by to fine structure constant. Despite the smallness of this contribution the theoretical understanding is important for a total estimation of the full SM result.

In the present paper the light-by-light contribution of axial-vector particles is considered in the framework of the nonlocal quark model. The paper is continuation of quark model estimations of LbL contributions. The LbL contributions to the anomalous magnetic moment of muon the light pseudoscalar and scalar resonances exchanges and the dynamical quark loop, i.e. contact type, within the nonlocal chiral quark model is calculated in [7–9]. In the present work we extend our model calculations by including the vector–axial-vector sector<sup>1</sup>. For this reason the

<sup>1</sup> It is interesting to note that in [10] is shown that the axial-vector exchange interaction in muonic hydrogen gives essential contribution to hyperfine splitting. For hyperfine splitting the axial-vector contribution is even bigger than the pion one [11].

model parameters should be refitted to the pion observables, the mixing of the pseudoscalar and longitudinal part of the axial-vector mesons as well as to the  $\rho - \gamma$  mixing. Preliminary results are given in [12].

The structure of paper is following. In Sec. II the nonlocal model is discussed. Only nonstrange mesons are considered. In Sec. III the interactions with external conserved currents is introduced. In Sec. IV the two-photon transition form-factors of pseudoscalar and axial-vector meson are considered. The Sec. V is devoted to discussion of model parameters. In Sec. VI the procedure of calculating of light-by-light contribution from transition form-factors is represented. The result of our calculations is given in Sec. VII and in Sec. VIII there is a comparison with other approaches. The conclusions are given in Sec. IX.

## II. MODEL

The nonlocal chiral quark model with light quarks and the pseudoscalar–scalar and vector–axial-vector sectors is considered and Lagrangian of model has the form

$$\begin{aligned} \mathcal{L} &= \mathcal{L}_{free} + \mathcal{L}_{P,S} + \mathcal{L}_{V,A}, \quad \mathcal{L}_{free} = \bar{q}(x)(i\hat{\partial} - m_c)q(x), \\ \mathcal{L}_{P,S} &= \frac{G_1}{2} \left( [J_S^a(x)]^2 + [J_P^a(x)]^2 \right), \quad \mathcal{L}_{V,A} = \frac{G_2}{2} \left( [J_V^{a,\mu}(x)]^2 + [J_A^{a,\mu}(x)]^2 \right), \end{aligned} \quad (4)$$

where  $m_c$  is the current quark mass matrix with diagonal elements  $m_c^u = m_c^d$ ,  $G_1$  and  $G_2$  are the coupling constants in pseudoscalar–scalar (P,S) and vector–axial-vector sectors (V,A), respectively. The nonlocal quark currents are given by <sup>2</sup>

$$J_M^{a\{\mu\}}(x) = \int d^4x_1 d^4x_2 f(x_1) f(x_2) \bar{q}(x - x_1) \Gamma_M^{a\{\mu\}} q(x + x_2), \quad (5)$$

with  $M = S, P, V, A$  and  $\Gamma_S^a = \lambda^a$ ,  $\Gamma_P^a = i\gamma^5 \lambda^a$ ,  $\Gamma_V^{a,\mu} = \gamma^\mu \lambda^a$ ,  $\Gamma_A^{a,\mu} = \gamma^5 \gamma^\mu \lambda^a$ . For the  $SU(2)$  model, the flavour matrices are  $\lambda^a \equiv \tau^a$ ,  $a = 0, \dots, 3$  with  $\tau^0 = 1$ . In Eq. (5),  $f(x)$  is the form factor reflecting the nonlocal properties of the QCD vacuum. Since only four-quark interaction is considered the action of the model can be bosonized by the usual Hubbard-Stratonovich trick with introduction of auxiliary mesonic fields for each quark current, i.e.  $P, S, V, A$ . The resulting effective Lagrangian after spontaneous symmetry breaking can be written in the form

$$\begin{aligned} \mathcal{L}_{eff} &= \bar{q}(x)(i\hat{\partial}_x - m_c)q(x) + \sigma_0 J_S^0(x) - \frac{1}{2G_1} \left( [P^a(x)]^2 + [\tilde{S}^a(x) + \sigma_0]^2 \right) - \\ &- \frac{1}{2G_2} \left( [V^{a,\mu}(x)]^2 + [A^{a,\mu}(x)]^2 \right) + P^a(x) J_P^a(x) + \tilde{S}^a(x) J_S^a(x) + \\ &+ V_\mu^a(x) J_V^{a,\mu}(x) + A_\mu^a(x) J_A^{a,\mu}(x). \end{aligned} \quad (6)$$

The scalar isoscalar field has a nonzero vacuum expectation value  $\langle S^0 \rangle_0 = \sigma_0 \neq 0$ . The shift of the scalar isoscalar field  $S^0 = \tilde{S}^0 + \sigma^0$  in order to obtain a physical scalar field with zero vacuum expectation value leads to appearance of the dynamical quark mass which is depend on quark momentum<sup>3</sup> ( $m_{dyn} = -\sigma^0$ )

$$m(p) = m_c + m_{dyn} f^2(p), \quad m_{dyn} = G_1 \frac{8N_c}{(2\pi)^4} \int d_E^4 k \frac{f^2(k^2) m(k^2)}{k^2 + m^2(k^2)}, \quad (7)$$

and quark propagator is

$$S(p) = (\hat{p} - m(p))^{-1}. \quad (8)$$

Meson propagators can be obtained by taking quadratic terms over the meson field from Lagrangian at one loop level. For spin-0 mesons unrenormalized propagators are

$$D_M(p^2) = \frac{1}{-G_1^{-1} + \Pi_{MM}(p^2)} = \frac{g_M^2(p^2)}{p^2 - M_M^2}, \quad (9)$$

<sup>2</sup> Such structure of interaction correspond to those from instanton liquid model [13] (ILM).

<sup>3</sup> The same symbols are taken for Fourier-transformed functions.

meson masses are located at points  $p^2 = M_M^2$ , which corresponds to solution of equation

$$-G_1^{-1} + \Pi_{MM}(M_M^2) = 0,$$

and value of meson coupling constant on-mass shell  $g_M(M_M^2)$  can be obtained from (9) with l'Hôpital's rule. After redefinition of meson fields the spin-0 propagator has usual form

$$D_M^R(p^2) = D_M(p^2)/g_M^2(p^2) = (p^2 - M_M^2)^{-1}. \quad (10)$$

The quark polarization loops are

$$\Pi_{M_1 M_2}(p^2) = i \frac{N_c}{(2\pi)^4} \int d^4 k f^2(k_+) f^2(k_-) \text{Tr}_{d,f} [S(k_-) \Gamma_{M_1}^a S(k_+) \Gamma_{M_2}^b],$$

where  $k_{\pm} = k \pm p/2$  and trace is taken over Dirac and flavor matrices.

Quark loops and propagators of vector and axial-vector mesons should be divided to longitudinal and transversal part

$$D_M^{\alpha\beta}(p^2) = D_M^T(p^2) P_p^{T;\alpha\beta} + D_M^L(p^2) P_p^{L;\alpha\beta}, \quad (11)$$

with help of corresponding projectors

$$P_p^{T;\alpha\beta} = g^{\alpha\beta} - \frac{p^\alpha p^\beta}{p^2}, \quad P_p^{L;\alpha\beta} = \frac{p^\alpha p^\beta}{p^2}.$$

Transversal components corresponds to spin-1 states and unrenormalized propagators are

$$D_{V,A}^T(p^2) = \frac{1}{-G_2^{-1} + \Pi_{V,AA}^T(p^2)} = \frac{g_{V,A}^2(p^2)}{M_{V,A}^2 - p^2}, \quad (12)$$

renormalized propagators are  $D_M^{T;R}(p^2) = D_M^T(p^2)/g_M^2(p^2)$  and masses can be found from solution of

$$-G_2^{-1} + \Pi_{V,A}^T(M_{V,A}^2) = 0. \quad (13)$$

The meson vertex functions without mixing in momentum space are

$$\Gamma_{p_+, p_-}^{M\{\mu\}} = g_M(p^2) \Gamma_M^{\{\mu\}} f(p_-) f(p_+), \quad (14)$$

where  $p_{\pm}, k$  are the quark and meson momenta, respectively.

Longitudinal components are related with spin zero. In the case of system pseudoscalar–axial-vector states appears mixing [14, 15] due to quark polarization loop with pseudoscalar and axial-vector vertices

$$\Pi_{PA}^\mu(p^2) = p^\mu \Pi_{\pi a_1}(p^2), \quad (15)$$

and physical states can be found as solution of matrix equation [16]

$$\begin{aligned} \tilde{D}_P(p^2) &= \frac{-G_2^{-1} + \Pi_{AA}^L(p^2)}{\mathcal{D}(p^2)}, \quad \tilde{D}_{PA}(p^2) = \frac{\Pi_{PA}(p^2)}{\mathcal{D}(p^2)}, \quad \tilde{D}_A^L(p^2) = \frac{-G_1^{-1} + \Pi_{PP}(p^2)}{\mathcal{D}(p^2)}, \\ \mathcal{D}(p^2) &= [-G_1^{-1} + \Pi_{PP}(p^2)] [-G_2^{-1} + \Pi_{AA}^L(p^2)] - p^2 \Pi_{PA}^2(p^2), \quad \tilde{D}_{PA}^\mu(p^2) = p^\mu \tilde{D}_{\pi a_1}(p^2). \end{aligned} \quad (16)$$

One can represent the mixing (16) as modification of the pion vertex with the contribution of longitudinal component of axial-vector mesons

$$\Gamma_{p_+, p_-}^\pi = i\gamma^5 \lambda^a (g_\pi(p^2) - \hat{p} \tilde{g}_\pi(p^2)) f(p_-) f(p_+). \quad (17)$$

The pion coupling constants can be obtained from comparison of  $T$ -matrix elements from (17) and solution of system (16)

$$\frac{g_\pi^2(p^2)}{p^2 - M_\pi^2} = \tilde{D}_P(p^2), \quad \frac{g_\pi(p^2) \tilde{g}_\pi(p^2)}{p^2 - M_\pi^2} = \tilde{D}_{PA}(p^2), \quad (18)$$

after that the rest contribution of longitudinal part of axial-vector meson is simply

$$\tilde{D}_A^L(p^2) - p^2 \frac{\tilde{g}_\pi^2(p^2)}{p^2 - M_\pi^2} = \frac{1}{-G_2^{-1} + \Pi_{AA}^L(p^2)} = D_A^L(p^2), \quad (19)$$

i.e. all mixing is “eaten” by modification of pion vertex.

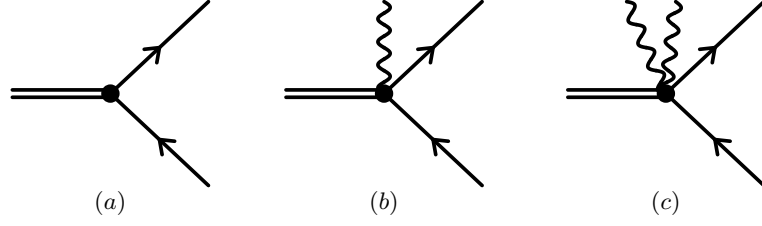


FIG. 1. Meson–quark–antiquark vertices: without photon (a), with one photon (b) and with two photons (c).

### III. EXTERNAL CURRENTS

Due to nonlocality the interactions with gauge electromagnetic field should be introduced not only to quark kinetic part but also to the nonlocal quark currents. Thus, in the presence of external gauge fields quark currents Eq. (5) takes the form

$$J_M^{\alpha\{\mu\}}(x) = \int d^4x_1 d^4x_2 f(x_1) f(x_2) \bar{Q}(x - x_1, x) \Gamma_M^{\alpha\{\mu\}} Q(x, x + x_2), \quad (20)$$

where the Schwinger phase factor is attached to each quark field  $Q(x, x + x_2) = E(x, x + x_2)q(x + x_2)$

$$E(x, y) = \mathcal{P} \exp \left\{ -iQ \int_x^y du_\mu G^\mu(u) \right\}, \quad (21)$$

where  $G^\mu$  is photon field and  $Q$  is charge matrix of quark fields. Unfortunately, the Ward identity fixed only longitudinal part of photon vertex and in order to find expression for the transversal part of vertices one need to specify rules for the contour integral. One of possible ways is the usage straight-path ansatz [17–19]  $z^\mu = x^\mu + \alpha(y^\mu - x^\mu)$ ,  $0 \leq \alpha \leq 1$ . An alternative scheme [20] which is used in this paper is based on the rules according to which the derivative of the contour integral does not depend on the form of the path and the explicit form of the path is not important

$$\frac{\partial}{\partial y^\mu} \int_x^y dz^\nu F_\nu(z) = F_\mu(y), \quad \delta^{(4)}(x - y) \int_x^y dz^\nu F_\nu(z) = 0.$$

The important feature of such prescriptions is that resulting expression for diagrams with nonlocal vertices will be expressed through finite-differences with momenta of diagrams with local vertices.

Since the Schwinger phase gauge factor contains field in exponent, vertices with arbitrary number of photon field can be generated. Due to the nonlocal interaction mesons with quarks, Fig. 1a, the vertices with one or two photons, Fig. 1bc, takes the form

$$\begin{aligned} \Gamma_{p_2, p_1, q_1}^{M\gamma; \{\alpha\}\mu} &= -g_M(k) \left( J_1^\mu(p_2, -q_1) Q \Gamma_M^{\alpha\{\mu\}} f(p_2) + f(p_2) \Gamma_M^{\alpha\{\mu\}} Q J_1^\mu(p_1, q_1) \right), \\ \Gamma_{p_2, p_1, q_1, q_2}^{M\gamma\gamma; \{\alpha\}\mu\nu} &= g_M(k) \left( J_2^{\mu\nu}(p_2, -q_1, -q_2) Q^2 \Gamma_M^{\alpha\{\mu\}} f(p_1) + J_1^\mu(p_2, -q_1) Q \Gamma_M^{\alpha\{\mu\}} Q J_1^\nu(p_1, q_2) + \right. \\ &\quad \left. + J_1^\nu(p_2, -q_2) Q \Gamma_M^{\alpha\{\mu\}} Q J_1^\mu(p_1, q_1) + f(p_2) \Gamma_M^{\alpha\{\mu\}} Q^2 J_2^{\mu\nu}(p_1, q_1, q_2) \right), \\ J_1^\mu(p, q) &= (2p + q)^\mu f_{p+q, p}^{(1)}, \\ J_2^{\mu\nu}(p, q_1, q_2) &= +2g^{\mu\nu} f_{p, p+q_1+q_2}^{(1)} + (2p + q_1)^\mu (2p + 2q_1 + q_2)^\nu f_{p, p+q_1, p+q_1+q_2}^{(2)} + \\ &\quad + (2p + q_2)^\nu (2p + 2q_2 + q_1)^\mu f_{p, p+q_2, p+q_1+q_2}^{(2)}, \end{aligned} \quad (22)$$

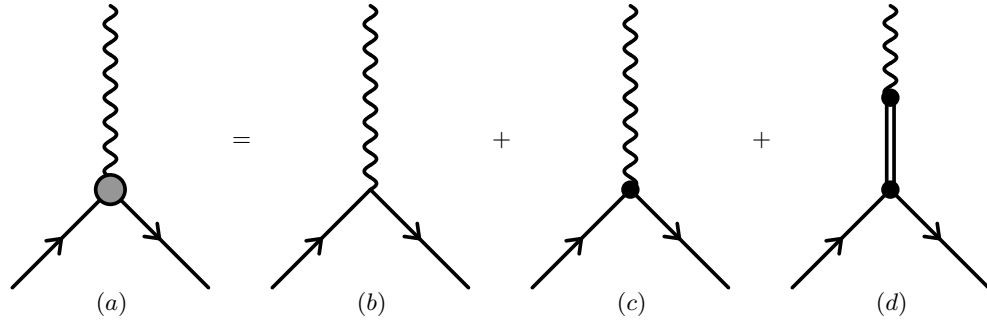


FIG. 2. Quark–antiquark–photon vertices : full (a), with local vertex (b), with nonlocal vertex (c) and with vector meson–photon transition (d).

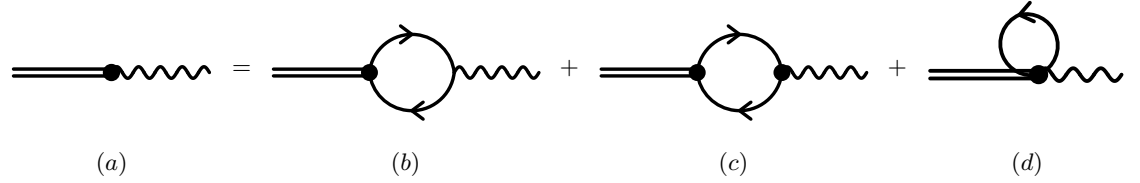


FIG. 3. Vector meson–photon mixing diagrams: total (a), with local vertex (b) and with nonlocal vertices (c), (d).

where the shorthand notations for first and second order finite-differences is introduced<sup>4</sup>

$$f_{p,q}^{(1)} = \frac{f(p) - f(q)}{p^2 - q^2}, \quad f_{p,q,l}^{(2)} = \frac{f_{p,q}^{(1)} - f_{p,l}^{(1)}}{q^2 - l^2}.$$

The terms with vacuum expectation of scalar field generate antiquark-quark-photon(s) vertices which can be rewritten from expression for scalar current (22) by using Eq. (7) in terms of quark mass

$$\begin{aligned} \Gamma_{p_2,p_1,q}^{\gamma;\mu} &= Q \left( \gamma_\mu - (p_1 + p_2)_\mu m_{p_1,p_2}^{(1)} \right), \\ \Gamma_{p_2,p_1,q_1,q_2}^{\gamma\gamma;\mu\nu} &= Q^2 \left( 2g^{\mu\nu} m_{p_1,p_2}^{(1)} + (2p_1 + q_1)^\mu (2p_2 - q_2)^\nu m_{p_1,p_1+q_1,p_2}^{(2)} \right. \\ &\quad \left. + (2p_1 + q_2)^\nu (2p_2 - q_1)^\mu m_{p_1,p_1+q_2,p_2}^{(2)} \right). \end{aligned} \quad (23)$$

In the presence of the vector sector, an additional dressing of quark interaction vertices with photons arises due to  $\rho(\omega) \rightarrow \gamma$  transition [18, 21], see Fig.3. This transition is transversal and can be represented in the form

$$C_{\gamma V}(q^2) = iN_c \frac{P_q^{T;\mu\nu}}{3} \int \frac{d^4 k}{(2\pi)^4} \left\{ \text{Tr} \left[ S(k_+) \Gamma_{k_+,k_-,q}^{\gamma;\mu} S(k_-) \Gamma_{k_-,k_+}^{V;\nu} \right] + \text{Tr} \left[ \Gamma_{k,k,q}^{M\gamma;\mu\nu} S(k) \right] \right\}, \quad (24)$$

where  $V$  stands for  $\rho_0$  or  $\omega$  mesons. Transition diagram has feature  $C_{\gamma V}(0) = 0$  [18] and does not lead to photon mass or renormalization of quark charge [21].

One can understand effect of dressing on diagram level by joining Fig. 3 to the Fig. 1a or Fig. 1b in order to obtain full expression for vertices with one or two photons

$$\begin{aligned} \Gamma_{p_2,p_1,q}^{\gamma;\mu} &= \Gamma_{p_2,p_1,q}^{\gamma;\mu} + \sum_{V=\rho^0,\omega} \Gamma_{p_2,p_1}^{V;\alpha} P_q^{T;\alpha\mu} C_{\gamma V}(q), \\ \Gamma_{p_2,p_1,q_1,q_2}^{\gamma\gamma;\mu\nu} &= \Gamma_{p_2,p_1,q_1,q_2}^{\gamma\gamma;\mu\nu} + \sum_{V=\rho^0,\omega} \Gamma_{p_2,p_1,q_1}^{V\gamma;\alpha\nu} P_{q_1}^{T;\alpha\mu} C_{\gamma V}(q_1) + \sum_{V=\rho^0,\omega} \Gamma_{p_2,p_1,q_2}^{V\gamma;\alpha\mu} P_{q_2}^{T;\alpha\nu} C_{\gamma V}(q_2). \end{aligned} \quad (25)$$

<sup>4</sup> The similar abbreviations will be used for finite differences of mass function  $m \rightarrow m^{(i)}$ .

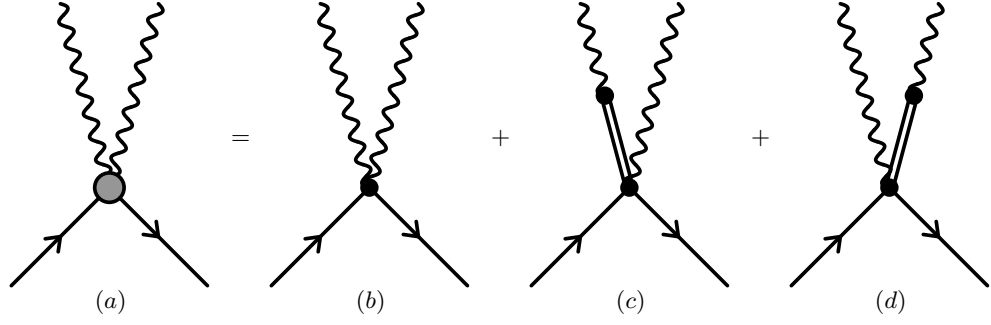


FIG. 4. Quark–antiquark–photon–photon vertices: with nonlocal vertex (b) and with vector meson–photon transition (c), (d).

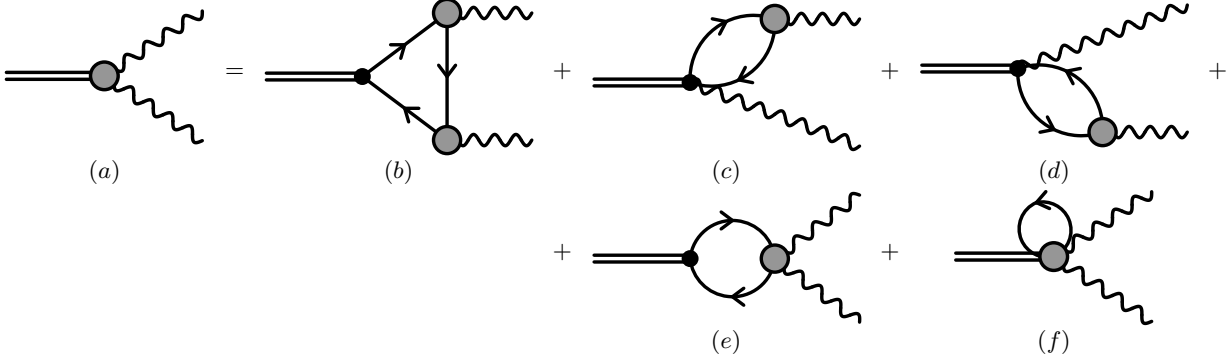


FIG. 5. Diagrams for meson transition form-factor: quark triangle (b) and with meson–photon–quark–antiquark vertex transition (c), (d), quark–antiquark–two–photon (e) and meson–quark–antiquark–two–photon (f).

#### IV. AV FORM-FACTOR

The transition form-factor of pseudoscalar meson has one structure

$$T^{\mu\nu}(p, q_1, q_2) = e^2 \Delta_P^{\mu\nu}(p, q_1, q_2), \quad \Delta_P^{\mu\nu}(p, q_1, q_2) = \varepsilon_{\mu\nu\rho\sigma} q_1^\rho q_2^\sigma F_P(p^2; q_1^2, q_2^2), \quad (26)$$

where  $p$  is momentum of virtual meson and two photons has momenta  $q_{1,2}$ .

The general form of the axial-vector meson to two-photon transition form factor is [22, 23]

$$T_\alpha^{\mu\nu}(p, q_1, q_2) = e^2 \Delta_{A,\alpha}^{\mu\nu}(p, q_1, q_2), \quad \Delta_{A,\alpha}^{\mu\nu}(p, q_1, q_2) = i\varepsilon_{\rho\sigma\tau\alpha} \sum_{i=1}^6 A_i(p^2, q_1^2, q_2^2) B_i^{\mu\nu\rho\sigma\tau}$$

$$B_1 = q_1^\tau g^{\mu\rho} g^{\sigma\nu}, \quad B_2 = q_2^\tau g^{\mu\rho} g^{\sigma\nu}, \quad B_3 = q_1^\nu q_1^\rho q_2^\sigma g^{\tau\mu}$$

$$B_4 = q_2^\nu q_1^\rho q_2^\sigma g^{\tau\mu}, \quad B_5 = q_1^\mu q_1^\rho q_2^\sigma g^{\tau\nu}, \quad B_6 = q_2^\mu q_1^\rho q_2^\sigma g^{\tau\nu} \quad (27)$$

where  $p$ ,  $q_1$  and  $q_2$  are momenta of AV meson and photons with indices  $\alpha, \mu, \nu$ . The gauge invariance provides the relations

$$A_2(p^2, q_1^2, q_2^2) = (q_1 \cdot q_2) A_6(p^2, q_1^2, q_2^2) + q_1^2 A_5(p^2, q_1^2, q_2^2),$$

$$A_1(p^2, q_1^2, q_2^2) = (q_1 \cdot q_2) A_3(p^2, q_1^2, q_2^2) + q_2^2 A_4(p^2, q_1^2, q_2^2) \quad (28)$$

and the Bose symmetry leads to

$$A_1(p^2, q_1^2, q_2^2) = -A_2(p^2, q_2^2, q_1^2), \quad A_3(p^2, q_1^2, q_2^2) = -A_6(p^2, q_2^2, q_1^2),$$

$$A_4(p^2, q_1^2, q_2^2) = -A_5(p^2, q_2^2, q_1^2). \quad (29)$$

Longitudinal to meson momentum piece of amplitude is

$$\Delta_{A,\alpha;L}^{\mu\nu}(p, q_1, q_2) = i\varepsilon^{\rho\sigma\mu\nu} q_{1\rho} q_{2\sigma} p_\alpha \frac{1}{p^2} \left( A_2(p^2, q_1^2, q_2^2) - A_1(p^2, q_1^2, q_2^2) \right). \quad (30)$$

The transversal part of amplitude can be rewritten as<sup>5</sup> [29]

$$\begin{aligned} \Delta_{A,\alpha}^{\mu\nu}(p, q_1, q_2) &= i\varepsilon_{\rho\sigma\tau\alpha} R_{q_1, q_2}^{\mu\rho} R_{q_1, q_2}^{\nu\sigma} (q_1 - q_2)^\tau (q_1 \cdot q_2) F_{A\gamma^*\gamma^*}^{(0)}(p^2, q_1^2, q_2^2) \\ &\quad + R_{q_1, q_2}^{\nu\rho} Q_1^\mu q_1^\sigma q_2^\tau F_{A\gamma^*\gamma^*}^{(1)}(p^2, q_1^2, q_2^2) + R_{q_1, q_2}^{\mu\rho} Q_2^\nu q_2^\sigma q_1^\tau F_{A\gamma^*\gamma^*}^{(1)}(p^2, q_2^2, q_1^2) \Big\}, \\ R_{q_1, q_2}^{\mu\nu} &= -g^{\mu\nu} + \frac{1}{X} \left\{ (q_1 \cdot q_2) (q_1^\mu q_2^\nu + q_2^\mu q_1^\nu) - q_1^2 q_2^\mu q_2^\nu - q_2^2 q_1^\mu q_1^\nu \right\}, \\ Q_1^\mu &= q_1^\mu - q_2^\mu \frac{q_1^2}{(q_1 \cdot q_2)}, \quad Q_2^\nu = q_2^\nu - q_1^\nu \frac{q_2^2}{(q_1 \cdot q_2)}, \quad X = (q_1 \cdot q_2)^2 - q_1^2 q_2^2, \end{aligned} \quad (31)$$

where  $R_{q_1, q_2}^{\mu\nu}$  is the totally transverse tensor,  $Q_1^\mu$  and  $Q_2^\nu$  are transverse with respect to  $q_1$  and  $q_2$ , respectively<sup>6</sup>. After projecting to the transversal components and using Shouten identity one can relate (27) and (31) as<sup>7</sup>

$$\begin{aligned} F_{A\gamma^*\gamma^*}^{(0)} &= \frac{(q_1^2 + (q_1 \cdot q_2))A_1 + ((q_1 \cdot q_2) + q_2^2)(q_1^2 A_5 + (q_1 \cdot q_2)A_6)}{(q_1 \cdot q_2)(q_1^2 - q_2^2)}, \\ F_{A\gamma^*\gamma^*}^{(1)} &= -\frac{(q_1 \cdot q_2)}{X} \left( A_1 + (q_1 \cdot q_2)A_5 + q_2^2 A_6 \right). \end{aligned} \quad (33)$$

where arguments of functions  $A_i$  are  $(p^2, q_1^2, q_2^2)$ .

According to the Landau–Yang theorem [31, 32], the axial-vector mesons can not decay into two real photons. However, the coupling of  $1^{++}$  mesons to two photons is allowed in the case when one or both photons are virtual. The two-photon “decay” width for axial-vector meson is defined for one quasireal longitudinal photon and real photon as

$$\tilde{\Gamma}_{\gamma\gamma}(A) = \lim_{Q^2 \rightarrow 0} \frac{1}{2} \frac{M_A^2}{Q^2} \Gamma(A \rightarrow \gamma_T \gamma_L^*) = \frac{\pi \alpha^2 M_A^5}{12} [F_{A\gamma^*\gamma^*}^{(1)}(M_A^2, 0, 0)]^2. \quad (34)$$

In quark model the photon-meson transition amplitude is a sum of diagrams shown in Fig. 5. The general expression for quark loop integral takes the form

$$\begin{aligned} \Delta_{M, \{\alpha\}}^{\mu\nu}(p, q_1, q_2) &= -iN_c \int \frac{d^4 k}{(2\pi)^4} \text{Tr} \left( 2\mathbf{\Gamma}_{k_2, k_1}^{M; \{\alpha\}} \mathbf{S}(k_1) \mathbf{\Gamma}_{k_1, k_3, q_1}^{\gamma; \mu} \mathbf{S}(k_3) \mathbf{\Gamma}_{k_3, k_2, q_2}^{\gamma; \nu} \mathbf{S}(k_2) + \right. \\ &\quad + \mathbf{\Gamma}_{k_2, k_3, q_1}^{M\gamma; \{\alpha\} \mu} \mathbf{S}(k_3) \mathbf{\Gamma}_{k_3, k_2, q_2}^{\gamma; \nu} \mathbf{S}(k_2) + \mathbf{\Gamma}_{k_3, k_1, q_2}^{M\gamma; \{\alpha\} \nu} \mathbf{S}(k_1) \mathbf{\Gamma}_{k_1, k_3, q_1}^{\gamma; \mu} \mathbf{S}(k_3) \\ &\quad \left. + \mathbf{\Gamma}_{k_2, k_1}^{M; \{\alpha\}} \mathbf{S}(k_1) \mathbf{\Gamma}_{k_1, k_2, q_1, q_2}^{\gamma\gamma; \mu\nu} \mathbf{S}(k_2) + \mathbf{\Gamma}_{k_3, k_3, q_1, q_2}^{M\gamma\gamma; \{\alpha\} \mu\nu} \mathbf{S}(k_3) \right), \end{aligned} \quad (35)$$

where the symbols are the photon momenta  $q_{1,2}$ , the meson momentum  $p = q_1 + q_2$ , and the quark momenta  $k_{1,2,3}$  ( $k_1 = k + q_1$ ,  $k_2 = k - q_2$ ,  $k_3 = k$ ). The first term in parentheses corresponds to the quark triangle diagram Fig. 5b (factor 2 comes from crossed one) and next terms corresponds to the diagrams in Figs. 5c-f with effective nonlocal vertices.

## V. MODEL PARAMETERS

At first glance model parameters can be taken from [18] since our model is somewhat similar: only nonstrange particles with vector–axial-vector sector, form-factor in Gaussian form,  $f(k^2) = \exp(-k^2/\Lambda^2)$  in Euclidean space, and not included currents with derivatives which are leading to the quark wave function renormalization like in [33, 34].

However, it is better to investigate dependence on model parameters similarly to analysis in Refs. [8, 9]. Remind, that the model with only scalar-pseudoscalar sector has three parameters: the current quark mass  $m_{c,u}$ , the dynamical quark mass  $m_{d,u}$  and the nonlocality parameter  $\Lambda$ . In order to understand the stability of the model predictions with respect to changes of the model parameters one may vary dynamical quark mass in rather wide physically acceptable

<sup>5</sup> Different expressions for transition form-factor can be found in [24–30].

<sup>6</sup> Our definition is differs from [29] by factor  $M_A^2$ .

<sup>7</sup> The relation with scalar functions  $\mathcal{F}_i^A(q_1^2, q_2^2)$  of [28] are

$$\mathcal{F}_1^A = M_A^2(A_3 + A_6)/2, \quad \mathcal{F}_2^A = -M_A^2(A_3 + A_5), \quad \mathcal{F}_3^A = -M_A^2(A_4 + A_6) \quad (32)$$

TABLE I. Different parameterizations of model parameters  $\Lambda$ ,  $m_c$ ,  $m_d$ ,  $G_1$ ,  $G_2$ .

$m_d$ , MeV	$m_c$ , MeV	$\Lambda$ , GeV	$G_1$ , GeV <sup>-2</sup>	$G_2$ , GeV <sup>-2</sup>
293	7.12	1.066	30.602	-2.6405
300	7.28	1.045	32.345	-3.9895
310	7.72	1.005	35.947	-4.9753
320	8.24	0.9631	40.248	-5.6046
330	8.82	0.9223	45.205	-5.9805
340	9.48	0.8825	50.930	-6.0630
350	10.24	0.8425	57.765	-5.6044
354	10.64	0.8241	61.268	-4.8984

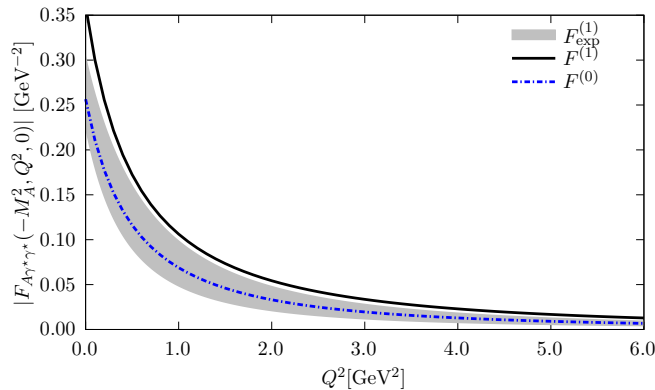


FIG. 6. Behaviour of the form-factors for  $f_1(1285)$  on mass-shell. Nonlocal model calculation: black solid line is  $-F_{A\gamma^*\gamma^*}^{(1)}(M_A^2, Q^2, 0)$ , blue dash-dotted is  $F_{A\gamma^*\gamma^*}^{(0)}(M_A^2, Q^2, 0)$ . Shaded region is the result of L3 collaboration for  $-F_{A\gamma^*\gamma^*}^{(1)}(M_A^2, Q^2, 0)$ .

interval 200–350 MeV, while fix other parameters by using as input the pion mass, the two-photon decay constant of the neutral pion. Inclusion of vector sector leads to appearance additional four-quark coupling constant  $G_2$  which can be fixed in favor of  $\rho$ -meson mass, Eq. 13. Unfortunately, the singularities of quark propagator restrict region for calculation of  $\rho$ -meson mass to 293 – 354 MeV. The model parameters for this region is given in table I where the ratio  $G_2/G_1$  is between  $-0.08$  and  $-0.14$ . In order to check sensitivity of the model to changes of parameters the calculation with fixed ratios  $G_2/G_1 = -0.08$ ,  $G_2/G_1 = -0.14$  is also performed in wider range of dynamical quark masses. The central value is taken for set of model parameters with  $m_d = 310$  MeV. For this parameter set one can calculate properties of  $A_1$  meson without any complications and ambiguities due to singularities of quark propagator. The  $A_1$  meson mass in model for this parameter set is found to be  $M_A = 918$  MeV. It is well-know the even in local NJL model the mass of axial meson is underestimated [14]. Thus there is a relation  $M_A^2 = M_\rho^2 + 6m^2$ , where  $m$  is constituent quark mass, and from this relation with experimental values of meson masses it should be around 400 MeV. It is more interesting to compare coupling of axial meson with two photons. At present, there are only few experimental data on the  $1^{++}$  meson transition form factor into two photons. The L3 Collaboration studied the reaction  $e^+e^- \rightarrow e^+e^-\gamma^*\gamma^* \rightarrow e^+e^-f_1(1285) \rightarrow e^+e^-\eta\pi^+\pi^-$  and the  $f_1(1285)$  meson transition form factor into pair photons where only one is real, was extracted [35]. The result for dipole form-factor fit is

$$\tilde{\Gamma}_{\gamma\gamma}(A) = 3.5 \pm 0.6 \pm 0.5 \text{ keV}, \quad \Lambda_{dip} = 1.04 \pm 0.06 \pm 0.05 \text{ GeV}. \quad (36)$$

The comparison of the model calculations for the axial-vector meson form factors with the results of the L3 collaboration is shown in fig. 6. One can see that for the kinematic when the meson is on mass shell, the agreement of the model calculation with the experiment is quite reasonable.



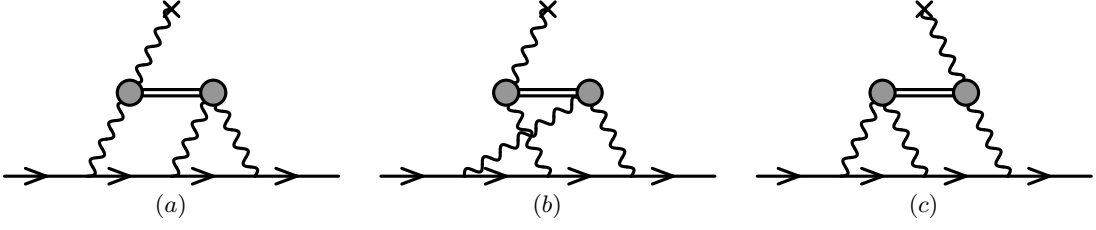


FIG. 7. LbL contribution from intermediate meson exchanges.

## VI. LBL CONTRIBUTION

The muon anomalous magnetic moment is defined from the following projection [36]

$$\begin{aligned}
 a_\mu^{\text{HLbL}} &= \frac{1}{48m_\mu} \text{Tr}((\hat{p} + m_\mu)[\gamma^\rho, \gamma^\sigma](\hat{p} + m_\mu)\Pi_{\rho\sigma}(p, p)), \\
 \Pi_{\rho\sigma}(p', p) &= -ie^6 \int \frac{d^4q_1}{(2\pi)^4} \int \frac{d^4q_2}{(2\pi)^4} \frac{1}{q_1^2 q_2^2 (q_1 + q_2 - k)^2} \times \\
 &\quad \times \gamma^\mu \frac{\hat{p}' - \hat{q}_1 + m_\mu}{(p' - q_1)^2 - m_\mu^2} \gamma^\nu \frac{\hat{p} - \hat{q}_1 - \hat{q}_2 + m_\mu}{(p - q_1 - q_2)^2 - m_\mu^2} \gamma^\lambda \frac{\partial}{\partial k^\rho} \Pi_{\mu\nu\lambda\sigma}(q_1, q_2, k - q_1 - q_2),
 \end{aligned} \tag{37}$$

where  $m_\mu$  is the muon mass, the static limit  $k_\mu \equiv (p' - p)_\mu \rightarrow 0$  is implied. Four-rank polarization tensor  $\Pi_{\mu\nu\lambda\sigma}$  is saturated by resonances, see fig. 7.

For pseudoscalar meson it is

$$\begin{aligned}
 \Pi^{\mu\nu\lambda\rho}(q_1, q_2, q_3) &= i\Delta_P^{\mu\nu}(q_1 + q_2, q_1, q_2) \frac{1}{(q_1 + q_2)^2 - M_P^2} \Delta_P^{\lambda\rho}(q_1 + q_2, q_3, q_4) + \\
 &\quad + i\Delta_P^{\mu\rho}(q_2 + q_3, q_1, q_4) \frac{1}{(q_2 + q_3)^2 - M_P^2} \Delta_P^{\nu\lambda}(q_2 + q_3, q_2, q_3) + \\
 &\quad + i\Delta_P^{\mu\lambda}(q_1 + q_3, q_1, q_3) \frac{1}{(q_1 + q_3)^2 - M_P^2} \Delta_P^{\nu\rho}(q_1 + q_3, q_2, q_4).
 \end{aligned} \tag{38}$$

Expression for other mesons can be rewritten in the same manner with corresponding changes of form-factors and propagators, i.e. the first line in (38) for axial-vector meson is

$$i\Delta_{A,\alpha}^{\mu\nu}(q_1 + q_2, q_1, q_2) \left( D_M^{T;R}(p^2) P_{q_1+q_2}^{T;\alpha\beta} + D_M^{L;R}(p^2) P_{q_1+q_2}^{L;\alpha\beta} \right) \Delta_{A,\beta}^{\lambda\rho}(q_1 + q_2, q_3, q_4). \tag{39}$$

Then, by averaging over the direction of muon momentum the result for  $a_\mu^{\text{HLbL}}$  becomes a three-dimensional integral with the radial variables of integration  $Q_1, Q_2$  and the angular variable [8, 37–40]. After integration over the angular variable the LbL contribution can be represented in the form [9]

$$a_\mu^{\text{LbL}} = \int_0^\infty dQ_1 \int_0^\infty dQ_2 \rho(Q_1, Q_2), \tag{40}$$

where  $\rho(Q_1, Q_2)$  is density function for contribution to  $g - 2$ . We cross-checked that in our program reproduced expression for projectors suggested in [37] as well as numerical results for pion pole [41].

## VII. RESULT

The result of calculation for LbL contribution of  $\pi$  with  $\pi - a_1$  mixed component and  $a_1 + f_1$  mesons is given in left part of fig. 8. Let us remind the case of ideal mixing is considered for  $a_1$  and  $f_1$  mesons. Partial contribution of transversal and longitudinal components of axial meson are shown in right part of fig. 8. Surprisingly, the most contribution comes from longitudinal part.

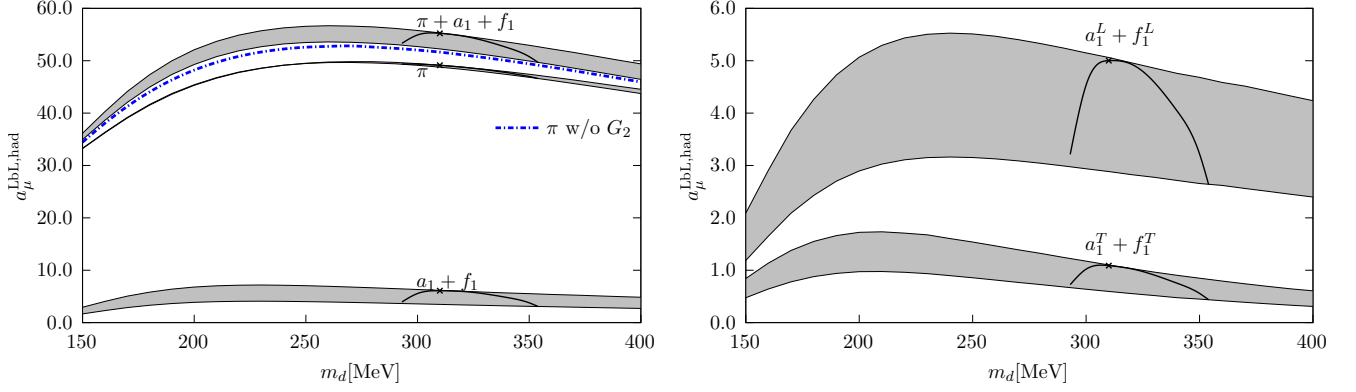


FIG. 8. (in units  $10^{-11}$ ) Left: LbL contribution to the muon AMM from the  $\pi$ ,  $a_1 + f_1$  and  $\pi + a_1 + f_1$  exchanges for different parameterizations as a function of the dynamical quark mass. The shaded area corresponds to region between fixing  $G_1/G_2 = -0.08$  and  $G_1/G_2 = -0.14$ . Black solid lines correspond to the parametrization when  $G_2$  is fixed in order to reproduce physical value of  $\rho$ -meson mass. Cross corresponds to result with  $m_d = 310$  MeV. Blue dash dotted line is pion contribution in model without vector sector [7]. Right: Separate contribution of longitudinal and transversal components of  $a_1 + f_1$  mesons for different parameterizations as a function of the dynamical quark mass.

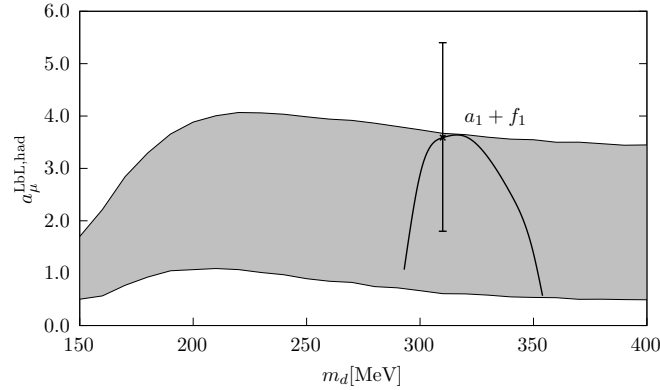


FIG. 9. (in units  $10^{-11}$ ) LbL contribution to the muon AMM from  $a_1 + f_1$  exchanges for different parameterizations as a function of the dynamical quark mass. The result is obtained as a difference of  $\pi + a_1 + f_1$  contribution in model with vector sector from pion contribution in model without spin-1 particles. Cross corresponds to result with  $m_d = 310$  MeV which is taken as central value and error bar is estimated as difference between highest and lowest values.

Analysis of axial meson contribution is complicated due to mixing of  $a_1$  meson with pion which leads to change of pion properties. Therefore, it is necessary to refit model parameters before perform the comparison. However, after the refitting of model parameters one can find that pion contribution in model without vector sector is differs from the model with it. Therefore, it seems more meaningful for a given dynamical quark mass to subtract from full  $\pi + a_1 + f_1$  contribution in model with vector sector the result of  $\pi$  contribution in model without vector sector. In such a way one can isolate just axial contribution and make it additive.

Let us illustrate situation for a set of model parameters with  $m_d = 310$  MeV since this set is used as a central point for estimations. The numbers are following: pion LbL contribution in model without vector sector 51.6,  $\pi + a_1 + f_1$  LbL contribution in model with vector sector 55.2, so the  $a_1 + f_1$  contribution is 3.6.

In order to understand ratio of transversal to longitudinal modes we used set with  $m_d = 310$  MeV without any normalization. For the error band is estimated as the difference between highest, i.e. for  $G_2/G_1 = -0.14$ , and lowest ( $G_2/G_1 = -0.08$ ) values of contribution. These are lines which restricts shaded region in fig. 9. Therefore, the estimation for  $a_1 + f_1$  contribution is  $3.6 \pm 1.8$ .

TABLE II. Contribution to  $a_\mu$  from axial-vector meson exchanges (in  $10^{-11}$ ). The  $a_1(1260)$ ,  $f_1(1285)$  and  $f_1(1420)$  mesons are denoted as  $a_1, f_1, f'_1$ . When it is possible the partial contributions of mesons is given in Note field in braces. T and L means transversal and longitudinal modes, correspondingly.

Ref.	Contribution	Note
[42, 43]	$2.5 \pm 1$	ENJL model
[44, 45]	$1.74 \pm 0.35$	ENJL model
[46]	$22 \pm 5$	Resonance+OPE, partial contributions $a_1, f_1, f'_1$ : $\{5.7 + 15.6 + 0.8\}$
[47]	$6.4 \pm 2$	Resonance, dipole FF from L3, partial contributions $f_1, f'_1$ : $\{5 + 1.4\}$
[38]	$7.55 \pm 2.71$	Resonance+OPE, partial contributions $a_1, f_1, f'_1$ : $\{1.89 + 5.19 + 0.47\}$
[48]	28	AdS/CFT, tower of resonances in channels $a_1, f_1, f'_1$ , partial T and L modes: $\{4 + 4 + 6\}$ and $\{4 + 4 + 6\}$
[49]	$22 \pm 5$	AdS/CFT, tower of resonances in channels $a_1, f_1, f'_1$ , partial T and L modes: $\{9\}$ and $\{13\}$
[50]	$0.8^{+3.5}_{-0.1}$	Resonance chiral theory, $a_1, f_1, f'_1$
[51]	27.8	AdS/CFT with the $U(1)_A$ anomaly, v1(OPE) fit, partial contributions $a_1, f_1, f'_1$ : $\{7.8 + 5.71 + 14.3\}$
	25	v1( $F_\rho$ -fit), partial contributions $a_1, f_1, f'_1$ : $\{7.1 + 4.34 + 13.6\}$
[52]	$15 \pm 10$	"Glasgow consensus"
[5]	$6 \pm 6$	WP 2020
This work	$3.6 \pm 1.8$	Ratio of T and L modes contribution: T/L= $\{0.22\}$

## VIII. DISCUSSION

In the nonlocal chiral quark model the result for contribution of  $a_1(1260)$  and  $f_1(1285)$  in case of ideal mixing is estimated as  $(3.6 \pm 1.8) \cdot 10^{-11}$ . This estimations includes full kinematic dependence of vertices, i.e. off-shell effects for mesonic bound state, revaluation of the pion contribution resulting due to  $\rho - \gamma$  and  $\pi - a_1$  mixings and refit of model parameters. Moreover, the estimation is also normalized to the model without vector sector, so result is this sense additive and could be compared with other estimations. For this purpose our result is presented in table II together with other estimations.

One can see that our result is comparable in size with

- early estimations in the NJL-like models [42–45]
- using form-factors from L3 collaboration data [47]
- resonances + OPE restriction [38]
- resonances chiral theory [49].

Our result is lower than

- Melnikov-Vainshtein estimations [46]
- AdS/CFT calculations with inclusion of tower of resonances [48] and [49].
- AdS/CFT calculations with the  $U(1)_A$  anomaly [51].

Our result is compatible "White Paper 2020" estimation [5].

## IX. CONCLUSIONS

The LbL contribution of axial-vector mesons to anomalous magnetic moment of muon is estimated in the framework of quark model. Inclusion of axial-vector particles leads to mixing with pseudoscalar states while vertices of interaction with photons are dressed by vector particles. The model parameters are refitted. In order to obtain final result the difference of contribution  $\pi + a_1 + f_1$  in model with vector sector is normalized to pion result in the model without vector sector.

In nonlocal quark model the transition form-factors of meson depend not only virtuality of photons but also on virtuality of meson. This leads to strong decrease and resulting value for LbL contribution is  $(3.6 \pm 1.8) \cdot 10^{-11}$ . The effect of suppression of LbL contribution due to virtuality of meson is discussed for the case of  $\pi$ ,  $\eta$ ,  $\eta'$  mesons in [7].

On the other hand in quark model exist not only diagrams with mesonic resonances but also large contribution of dynamical quark loop, i.e. contact term. This contact contribution holds short range asymptotics [7, 9]. The similar situation should be in DSE approach [53]. Therefore, it is possible that total contribution will be somehow rearranged in different approaches.

Thus, for example, in five-dimensional model where fifth dimension is later integrated out and which mimics QCD in the large- $N_c$  limit [48] the short distance constrain is achieved through the infinite tower of axial-vector contribution of the  $a_1(1260)$ ,  $f_1(1285)$  and  $f_1^*(1420)$ .

Similarly, in the [49] the axial vector meson contributions arising from the Chern-Simons action in the holographic QCD models is estimated and it is found that the infinite tower of axial vector mesons leads to correct behavior at short distances.

Another question is about relative ratio of transversal (T) and longitudinal (L) modes contribution to  $a_\mu$ . In nonlocal model most of contribution comes from L mode:  $T/L$  ratio is only 0.22. In [48] the T and L contributions are the same while in [49] this ratio 0.7. Discussion of short-distance constrain, the longitudinal and transverse degrees of freedom of axial-vector mesons is given in [54]. It is interesting that result of only T mode contribution in nonlocal model  $3.6 \cdot 0.22 \sim 0.8$  similar to those obtained in resonance chiral theory [50].

In future we plan extend our calculations to the sector with strange particles and reestimate the influence of vector-axial-vector sector on the contact term (quark loop). Actually, the presence of the contact term is a main difference between models with quark degrees of freedom and pure mesonic one or the dispersive approach. Up to now, it is not clear how to relate these calculations since the mesonic contributions exist in both approaches, while the contact term is only attributed to the quark models. This contribution is small only for some models [42], while in calculation in the nonlocal model [9], the DSE/BSE approach [53], the model with quark box [55],  $C_\chi$ QM [56] this contribution is not small and even bigger than resonance one. Important to note, that in the nonlocal chiral quark model just the contact term guarantees the correct QCD asymptotics [7, 21].

*Authors thank A.E. Dorokhov, our friend and scientist, with whom we started this work.*

Diagrams are drawn with help of `feyn.gle` package [57]. The work is supported by Russian Science Foundation (grant No. RSF 23-22-00041).

- 
- [1] D. Hanneke, S. Fogwell, and G. Gabrielse, Phys. Rev. Lett. **100**, 120801 (2008), arXiv:0801.1134 [physics.atom-ph].
  - [2] G. W. Bennett *et al.* (Muon G-2 Collaboration), Phys. Rev. **D73**, 072003 (2006), arXiv:hep-ex/0602035 [hep-ex].
  - [3] B. Abi *et al.* (Muon g-2), Phys. Rev. Lett. **126**, 141801 (2021), arXiv:2104.03281 [hep-ex].
  - [4] T. Aoyama, T. Kinoshita, and M. Nio, Atoms **7**, 28 (2019).
  - [5] T. Aoyama *et al.*, Phys. Rept. **887**, 1 (2020), arXiv:2006.04822 [hep-ph].
  - [6] R. L. Workman *et al.* (Particle Data Group), PTEP **2022**, 083C01 (2022).
  - [7] A. Dorokhov, A. Radzhabov, and A. Zhevlakov, Eur. Phys. J. **C71**, 1702 (2011), arXiv:1103.2042 [hep-ph].
  - [8] A. Dorokhov, A. Radzhabov, and A. Zhevlakov, Eur. Phys. J. **C72**, 2227 (2012), arXiv:1204.3729 [hep-ph].
  - [9] A. E. Dorokhov, A. E. Radzhabov, and A. S. Zhevlakov, Eur. Phys. J. **C75**, 417 (2015), arXiv:1502.04487 [hep-ph].
  - [10] A. Dorokhov, N. Kochelev, A. Martynenko, F. Martynenko, and A. Radzhabov, Physics Letters B **776**, 105 (2018).
  - [11] A. E. Dorokhov, N. I. Kochelev, A. P. Martynenko, F. A. Martynenko, and R. N. Faustov, Phys. Part. Nucl. Lett. **14**, 857 (2017), 1704.07702v2.
  - [12] A. E. Dorokhov, A. P. Martynenko, F. A. Martynenko, A. E. Radzhabov, and A. S. Zhevlakov, EPJ Web Conf. **212**, 05001 (2019), arXiv:1910.07815 [hep-ph].
  - [13] A. E. Dorokhov and L. Tomio, Phys. Rev. **D62**, 014016 (2000).
  - [14] M. K. Volkov, Sov. J. Part. Nucl. **17**, 186 (1986).
  - [15] U. G. Meissner, Phys. Rept. **161**, 213 (1988).
  - [16] A. E. Kaloshin and A. E. Radzhabov, Phys. Atom. Nucl. **66**, 1375 (2003).
  - [17] R. D. Bowler and M. C. Birse, Nucl. Phys. **A582**, 655 (1995), arXiv:hep-ph/9407336 [hep-ph].
  - [18] R. S. Plant and M. C. Birse, Nucl. Phys. **A628**, 607 (1998).
  - [19] A. Scarpettini, D. Gomez Dumm, and N. N. Scoccola, Phys. Rev. **D69**, 114018 (2004), hep-ph/0311030.
  - [20] J. Terning, Phys. Rev. **D44**, 887 (1991).
  - [21] A. E. Dorokhov and W. Broniowski, Eur. Phys. J. **C32**, 79 (2003), hep-ph/0305037.
  - [22] L. Rosenberg, Phys. Rev. **129**, 2786 (1963).
  - [23] S. L. Adler, Phys. Rev. **177**, 2426 (1969).
  - [24] R. N. Cahn, Phys. Rev. **D35**, 3342 (1987).
  - [25] A. S. Rudenko, Phys. Rev. **D96**, 076004 (2017), 1707.00545v2.

- [26] A. A. Osipov, A. A. Pivovarov, and M. K. Volkov, Phys. Rev. D **96**, 054012 (2017), arXiv:1705.05711 [hep-ph].
- [27] A. Szczurek, Phys. Rev. D **102**, 113015 (2020), arXiv:2006.01516 [hep-ph].
- [28] M. Hoferichter and P. Stoffer, J. High Energy Phys. **05**, 159, arXiv:2004.06127 [hep-ph].
- [29] V. Pascalutsa, V. Pauk, and M. Vanderhaeghen, Phys. Rev. D **85**, 116001 (2012), arXiv:1204.0740 [hep-ph].
- [30] M. Zanke, M. Hoferichter, and B. Kubis, J. High Energy Phys. **07** (7), 106, arXiv:2103.09829 [hep-ph].
- [31] L. D. Landau, Dokl. Akad. Nauk SSSR **60**, 207 (1948).
- [32] C.-N. Yang, Phys. Rev. **77**, 242 (1950).
- [33] M. F. I. Villafañe, D. G. Dumm, and N. N. Scoccola, Phys. Rev. D **94**, 054003 (2016), arXiv:1602.06984 [hep-ph].
- [34] J. P. Carlomagno and M. F. I. Villafañe, Phys. Rev. D **100**, 076011 (2019), arXiv:1906.04257 [hep-ph].
- [35] P. Achard *et al.* (L3), Phys. Lett. **B526**, 269 (2002), arXiv:hep-ex/0110073 [hep-ex].
- [36] S. J. Brodsky and J. D. Sullivan, Phys. Rev. **156**, 1644 (1967).
- [37] F. Jegerlehner and A. Nyffeler, Phys.Rept. **477**, 1 (2009), arXiv:0902.3360 [hep-ph].
- [38] F. Jegerlehner, Springer Tracts Mod. Phys. **274**, pp.1 (2017).
- [39] G. Colangelo, M. Hoferichter, M. Procura, and P. Stoffer, J. High Energy Phys. **2015** (09), 074, arXiv:1506.01386 [hep-ph].
- [40] G. Colangelo, M. Hoferichter, M. Procura, and P. Stoffer, J. High Energy Phys. **2017** (04), 161, arXiv:1702.07347 [hep-ph].
- [41] M. Knecht and A. Nyffeler, Phys. Rev. **D65**, 073034 (2002).
- [42] J. Bijnens, E. Pallante, and J. Prades, Phys.Rev.Lett. **75**, 1447 (1995).
- [43] J. Bijnens, E. Pallante, and J. Prades, Nucl.Phys. **B474**, 379 (1996).
- [44] M. Hayakawa, T. Kinoshita, and A. I. Sanda, Phys. Rev. D **54**, 3137 (1996), arXiv:hep-ph/9601310 [hep-ph].
- [45] M. Hayakawa and T. Kinoshita, Phys. Rev. **D57**, 465 (1998), [Erratum: Phys.Rev.D 66, 019902 (2002)], arXiv:hep-ph/9708227 [hep-ph].
- [46] K. Melnikov and A. Vainshtein, Phys. Rev. **D70**, 113006 (2004).
- [47] V. Pauk and M. Vanderhaeghen, The European Physical Journal C **74**, 3008 (2014).
- [48] L. Cappiello, O. Catà, G. D'Ambrosio, D. Greynat, and A. Iyer, Phys. Rev. D **102**, 016009 (2020), arXiv:1912.02779 [hep-ph].
- [49] J. Leutgeb and A. Rebhan, Phys. Rev. D **101**, 114015 (2020), arXiv:1912.01596 [hep-ph].
- [50] P. Roig and P. Sanchez-Puertas, Phys. Rev. D **101**, 074019 (2020), arXiv:1910.02881 [hep-ph].
- [51] J. Leutgeb, J. Mager, and A. Rebhan 10.48550/ARXIV.2211.16562 (2022), arXiv:2211.16562 [hep-ph].
- [52] J. Prades, E. de Rafael, and A. Vainshtein, Adv. Ser. Direct. High Energy Phys. **20**, 303 (2009), arXiv:0901.0306 [hep-ph].
- [53] T. Goecke, C. S. Fischer, and R. Williams, Phys. Rev. **D83**, 094006 (2011), arXiv:1012.3886 [hep-ph].
- [54] P. Masjuan, P. Roig, and P. Sanchez-Puertas, J. Phys. G **49**, 015002 (2022), arXiv:2005.11761 [hep-ph].
- [55] A. A. Pivovarov, Phys. Atom. Nucl. **66**, 902 (2003).
- [56] D. Greynat and E. de Rafael, J. High Energy Phys. **2012** (7), 020, arXiv:1204.3029 [hep-ph].
- [57] A. Grozin, Comput. Phys. Commun. **283**, 108590 (2023), arXiv:2207.01351 [hep-ph].